

LONGITUDINAL STABILITY OF A COASTING BEAM IN A CORRUGATED RESISTIVE VACUUM CHAMBER

E. KEIL AND B. ZOTTER

ISR Division, CERN, Geneva, Switzerland

An analysis is made of the electromagnetic fields excited by longitudinal density fluctuations of an unbunched, relativistic particle beam drifting in a corrugated vacuum chamber of circular cross section. From these fields the coupling impedance is calculated, which is a measure of the reaction of an oscillating beam upon itself, and determines its stability. The coupling impedances of bellows and cross-section variations are investigated as functions of various geometric and beam parameters. Corrugations of a vacuum chamber may become resonant cavities at higher frequencies. The coupling impedance (divided by the mode number) may become several orders of magnitude larger than its value at lower frequencies, and severely endanger beam stability. The resonant coupling impedances can be found directly by computer solution of the matrix equations for the field coefficients.

INTRODUCTION

The increasing intensity in circular accelerators and especially storage rings causes growing concern about the stability of the circulating particle beam which is affected by the nature of the surroundings of the beam and has been described by well-known phenomena like the negative-mass instability⁽¹⁾ or the resistive-wall instability.⁽²⁾

Additional effects of this nature occur when the cross section of the vacuum chamber varies along the circumference of the machine. We investigate the effect of such corrugations on the longitudinal stability of an unbunched relativistic particle beam. We express our results in terms of the coupling impedance between the beam and its surroundings. Stability criteria for longitudinal oscillations have been expressed in this parameter.^(3,4) It has also been shown that the coupling impedance is equal to the shunt impedance⁽⁵⁾ which can be measured by rf techniques.

Section 1 contains the general field analysis for a model geometry shown in Fig. 1. The general solution for the electromagnetic field is obtained for the case where the tube connecting the cavities and the outer cavity wall have finite conductivity. The effect of finite conductivity of the cavity end walls can be approximately allowed for by augmenting the outer cavity resistivity in the ratio of the wall surfaces. The solution is formulated in compact matrix notation. The coupling impedance is defined in detail in 1.9.

Section 2 gives the effect of corrugations in the long wavelength limit. It turns out that each jump

in the cross section of the vacuum chamber adds an inductive term to the coupling impedance. In a large relativistic machine like the CERN Intersecting Storage Rings the total inductance due to the cross-section variations is about equal to the total resistive-wall effect, and much bigger than the capacitive negative-mass effect.

At higher frequencies the corrugations of the vacuum chamber become resonant cavities, and the coupling impedance may increase by their quality factor which is typically of the order of a few thousand. Section 3 is devoted to a detailed analysis of this resonant effect. Numerical results obtained by computer are shown in the form of graphs which give the resonant frequency, the coupling impedance and the quality factor for a wide range of cavity shapes. When the coupling impedance exceeds the permissible value, a beam instability may occur. Conversely, stability of circulating beams of a given intensity imposes an upper limit on the coupling impedance which must be achieved in the design of the machine by making the vacuum chamber sufficiently smooth and by damping the unavoidable resonant cavities to obtain sufficiently low values of the quality factors.

1. FIELD ANALYSIS OF A LONGITUDINALLY OSCILLATING PARTICLE BEAM IN A CORRUGATED VACUUM CHAMBER

1.1. The coupling impedance can be calculated from the electromagnetic fields generated by a perturbation on a beam of charged particles.

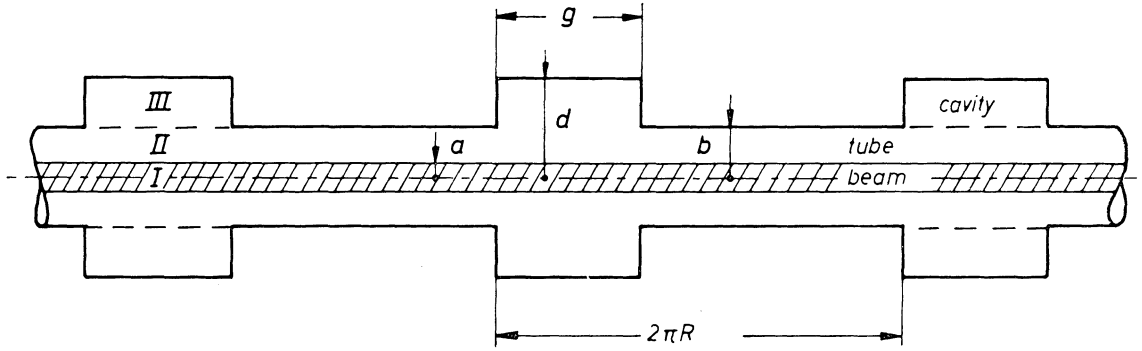


FIG. 1. Schematic cross-section of a few periods of the model geometry.

Since all pertinent equations are linear it is sufficient to investigate a sinusoidal longitudinal modulation of charge density with mode number n , i.e., with n wavelengths along the machine circumference. The perturbation wave travels with phase velocity βc . Thus its circular frequency is $\omega = \beta cn/R$. We shall neglect the small difference between the beam velocity and the phase velocity of the wave. We also neglect the curvature of the vacuum chamber which we replace by a straight periodic pipe with period $2\pi R$. We work in cylindrical coordinates as shown in Fig. 1: a cylindrical beam of radius a is surrounded by a concentric tube of radius b . Periodically, with distance $2\pi R$, the radius of the tube is enlarged to the value d over a length g .

1.2. The electromagnetic fields are found by solving the wave equation for the longitudinal electric field E_z :

$$\frac{1}{r} \frac{\partial}{\partial r} \left(r \frac{\partial E_z}{\partial r} \right) + \frac{\partial^2 E_z}{\partial z^2} + \frac{\omega^2}{c^2} E_z = \frac{1}{\epsilon} \frac{\partial \rho}{\partial z} - i\omega \mu J_z. \quad (1.1)$$

Here we have assumed that the time dependence of all waves is $\exp(-i\omega t)$. Because a centered beam with a density modulation only interacts with TM modes, we can limit our treatment to those modes and put $H_z = 0$. Derivatives with respect to ϕ in (1.1) vanish because of the rotational symmetry. The only nonvanishing transverse field components are given by

$$\begin{aligned} \left(\frac{\partial^2}{\partial z^2} + \frac{\omega^2}{c^2} \right) E_r &= \frac{\partial^2 E_z}{\partial r \partial z} \\ \left(\frac{\partial^2}{\partial z^2} + \frac{\omega^2}{c^2} \right) Z_0 H_\phi &= \frac{i\omega}{c} \frac{\partial E_z}{\partial r}. \end{aligned} \quad (1.2)$$

Here $Z_0 = (\mu_0/\epsilon_0)^{1/2} = 120\pi \Omega$ is the impedance of free space.

1.3. The right-hand side of the wave equation (1.1) differs from zero only in the beam region. We assume a density modulation

$$\rho = \hat{\rho} \exp [ik(z - \frac{1}{2}g)]$$

where $k = n/R$ is the axial wave number. The perturbed current density is, from the continuity equation, $J_z = \beta c \rho$. With $\epsilon = \epsilon_0$ and $\mu = \mu_0$, the rhs of (1.1) becomes

$$\frac{1}{\epsilon} \frac{\partial \rho}{\partial z} - i\omega \mu J_z = \frac{ik\hat{\rho}}{\epsilon_0 \gamma^2} \exp [ik(z - \frac{1}{2}g)], \quad (1.3)$$

where $\gamma = (1 - \beta^2)^{-1/2}$. We remove a factor $i\hat{\rho}/k\epsilon_0$ which otherwise would appear in all expressions for the fields. We then are left with $(k/\gamma)^2 \exp [ik(z - \frac{1}{2}g)]$ on the right-hand side, and we notice that $-\exp [ik(z - \frac{1}{2}g)]$ is a particular solution of (1.1).

1.4. We find the general solution of the homogeneous wave equation by separating the variables. We assume a solution in the form $E_z(r, z) = R(r)Z(z)$ and obtain two ordinary differential equations

$$\begin{aligned} \frac{1}{r} \frac{d}{dr} \left(r \frac{dR}{dr} \right) - \left(C^2 - \frac{\omega^2}{c^2} \right) R &= 0 \\ \frac{d^2 Z}{dz^2} + C^2 Z &= 0. \end{aligned} \quad (1.4)$$

The 'separation constant' C^2 must be chosen to fulfil the boundary conditions. The general solution is found by summing over all functions

belonging to the permissible values of C^2 , each multiplied by an arbitrary coefficient.

If we call the separation constant k_m the solutions of the axial equation (1.4) are

$$Z = \exp[\pm ik_m(z - \frac{1}{2}g)].$$

In order to have solutions that are periodic with $2\pi R$ we require $k_m = m/R$ where m is an arbitrary integer. The solutions of the radial equation are modified Bessel functions of order zero and argument $\chi_m r$ with $\chi_m^2 = k_m^2 - \omega^2/c^2$.

In the beam region I with $0 \leq r \leq a$, we must exclude the solution $K_0(\chi_m r)$ and thus we get $R(r) = I_0(\chi_m r)$. The complete solution is found by summing over all values of m , and by adding the particular solution of the inhomogeneous equation found above.

$$E_z^I = \sum_{m=-\infty}^{+\infty} [A_m I_0(\chi_m r) - \delta_{mn}] \exp[ik_m(z - \frac{1}{2}g)]. \quad (1.5)$$

Here we have used the Kronecker symbol δ_{mn} and the fact that $k = n/R = k_n$. The magnetic field component H_ϕ can be found using (1.3):

$$Z_0 H_\phi^I = -\frac{i\omega}{c} \sum_{m=-\infty}^{+\infty} \frac{A_m}{\chi_m} I_1(\chi_m r) \exp[ik_m(z - \frac{1}{2}g)]. \quad (1.6)$$

We notice that the fields are a superposition of an infinite number of terms with equally spaced axial wave numbers k_m . Such terms are typical for periodic systems and are usually called 'space harmonics'.

1.5. The solutions in the 'tube region' with $a \leq r \leq b$ differ from (1.5) and (1.6) only by the absence of the particular solution and by the presence of the $K_0(\chi_m r)$ terms:

$$E_z^{\text{II}} = \sum_{m=-\infty}^{+\infty} [B_m I_0(\chi_m r) + C_m K_0(\chi_m r)] \cdot \exp[ik_m(z - \frac{1}{2}g)] \quad (1.7)$$

$$Z_0 H_\phi^{\text{II}} = -\frac{i\omega}{c} \sum_{m=-\infty}^{+\infty} \frac{1}{\chi_m} [B_m I_1(\chi_m r) - C_m K_1(\chi_m r)] \cdot \exp[ik_m(z - \frac{1}{2}g)].$$

We can immediately reduce the number of unknown coefficients by requiring that the electric and magnetic fields at the beam edge $r = a$ be equal.

Equating term by term we can express B_m and C_m by A_m and thus obtain for the fields in region II:

$$E_z^{\text{II}} = \sum_m [A_m I_0(\chi_m r) + \chi a T_0(\chi r) \delta_{mn}] \cdot \exp[ik_m(z - \frac{1}{2}g)] \quad (1.8)$$

$$Z_0 H_\phi^{\text{II}} = -\frac{i\omega}{c} \sum_m \left[\frac{A_m}{\chi_m} I_1(\chi_m r) + a T_1(\chi r) \delta_{mn} \right] \cdot \exp[ik_m(z - \frac{1}{2}g)]$$

where $\chi^2 \equiv \chi_n^2 = k^2 - \omega^2/c^2 = k^2/\gamma^2$, and

$$T_i(\chi r) = -K_1(\chi a) I_i(\chi r) - (-)^i I_1(\chi a) K_i(\chi r). \quad (1.9)$$

They have the properties $T_0(\chi a) = -1/\chi a$ and $T_1(\chi a) = 0$ for any χ .

1.6. We assume that the end walls of the cavity are perfectly conducting and hence E_r must vanish at $z = 0$ and at $z = g$. The first condition implies sine solutions for E_r which, from (1.2), lead to cosine solutions for E_z . Calling the separation constant α_s^2 we find that the condition at $z = g$ is satisfied for $\alpha_s = s\pi/g$ where s is any positive integer or zero. The radial function again yields modified Bessel functions of order zero but with argument $\Gamma_s r$, where $\Gamma_s^2 = \alpha_s^2 - \omega^2/c^2$.

We write the most general solution for E_z and H_ϕ in the 'cavity region' with $b \leq r \leq d$ in the form

$$E_z^{\text{III}} = \sum_{s=0}^{\infty} [D_s R_0(\Gamma_s r) + D_s' S_0(\Gamma_s r)] \cos \alpha_s z$$

$$Z_0 H_\phi^{\text{III}} = -\frac{i\omega}{c} \sum_{s=0}^{\infty} \frac{1}{\Gamma_s} [D_s R_1(\Gamma_s r) + D_s' S_1(\Gamma_s r)] \cos \alpha_s z, \quad (1.10)$$

where

$$R_i(\Gamma r) = K_0(\Gamma d) I_i(\Gamma r) - (-)^i I_0(\Gamma d) K_i(\Gamma r)$$

$$S_i(\Gamma r) = -K_1(\Gamma d) I_i(\Gamma r) - (-)^i I_1(\Gamma d) K_i(\Gamma r). \quad (1.11)$$

For any Γ , we have $R_0(\Gamma d) = S_1(\Gamma d) = 0$ and $R_1(\Gamma d) = -S_0(\Gamma d) = 1/\Gamma d$.

The D_s and D_s' are as yet unknown coefficients. We can immediately eliminate D_s' by applying the boundary condition at $r = d$. Assuming that the outer cavity wall has conductivity σ_c we require to first order in \mathcal{R}_c :

$$E_z = -(1-i)\mathcal{R}_c Z_0 H_\phi, \quad (1.12)$$

where $\mathcal{R}_c = (\omega \epsilon_0 / 2\sigma_c)^{\frac{1}{2}}$ is the (dimensionless) normalized surface resistivity. It is related to the more

familiar skin depth δ_c by $\delta_c = 2c\mathcal{R}_c/\omega$. Combining (1.10) and (1.12) yields:

$$-\sum_s \frac{D_s'}{\Gamma_s d} \cos \alpha_s z = (1+i) \frac{\omega \mathcal{R}_c}{c} \sum_s \frac{D_s}{\Gamma_s^2 d} \cos \alpha_s z. \quad (1.13)$$

Equating term by term we find $D_s' = \eta_c D_s / \Gamma_s b$ where $\eta_c = (1+i)\omega b \mathcal{R}_c / c$. Therefore the field components (1.10) can be written in the form:

$$\begin{aligned} E_z^{\text{III}} &= \sum_{s=0}^{\infty} D_s \left[R_0(\Gamma_s r) - \frac{\eta_c}{\Gamma_s b} S_0(\Gamma_s r) \right] \cos \alpha_s z \\ Z_0 H_\phi^{\text{III}} &= -\frac{i\omega b}{c} \sum_{s=0}^{\infty} \frac{D_s}{\Gamma_s b} \\ &\quad \cdot \left[R_1(\Gamma_s r) - \frac{\eta_c}{\Gamma_s b} S_1(\Gamma_s r) \right] \cos \alpha_s z. \end{aligned} \quad (1.14)$$

1.7. The final step in the field calculation is the matching of the tangential field components at $r=b$. Assuming that the tube wall has finite conductivity σ_t we want to fulfil the conditions (\mathcal{R}_t and η_t are derived from σ_t as \mathcal{R}_c and η_c from σ_c):

$$\begin{aligned} E_z^{\text{II}}|_{r=b} &= E_z^{\text{III}}|_{r=b} & 0 < z < g \\ E_z^{\text{II}}|_{r=b} &= -(1-i)\mathcal{R}_t Z_0 H_\phi^{\text{II}}|_{r=b} & g < z < 2\pi R \\ H_\phi^{\text{II}}|_{r=b} &= H_\phi^{\text{III}}|_{r=b} & 0 < z < g. \end{aligned} \quad (1.15)$$

Introducing the abbreviations

$$\begin{aligned} \bar{A}_m &= A_m I_0(\chi_m b) \\ I_{mm} &= I_1(\chi_m b) / [\chi_m b I_0(\chi_m b)] \\ \bar{B}_m &= \chi a T_0(\chi b) \delta_{mn} \\ \bar{C}_m &= \frac{a}{b} T_1(\chi b) \delta_{mn} \\ \bar{D}_s &= D_s [R_0(\Gamma_s b) - \eta_c S_0(\Gamma_s b) / \Gamma_s b] \\ K_{ss} &= \frac{1}{\Gamma_s b} \frac{R_1(\Gamma_s b) - \eta_c S_1(\Gamma_s b) / \Gamma_s b}{R_0(\Gamma_s b) - \eta_c S_0(\Gamma_s b) / \Gamma_s b} \end{aligned} \quad (1.16)$$

we obtain the conditions

$$\begin{aligned} &\sum_{m=-\infty}^{+\infty} (\bar{A}_m + \bar{B}_m) \exp[ik_m(z - \frac{1}{2}g)] \\ &= \begin{cases} \sum_{s=0}^{\infty} \bar{D}_s \cos \alpha_s z & \text{for } 0 < g < z \\ \eta_t \sum_{m=-\infty}^{+\infty} (I_{mm} \bar{A}_m + \bar{C}_m) \exp[ik_m(z - \frac{1}{2}g)] & \text{for } g < z < 2\pi R \end{cases} \end{aligned}$$

$$\begin{aligned} &\sum_{m=-\infty}^{+\infty} (I_{mm} \bar{A}_m + \bar{C}_m) \exp[ik_m(z - \frac{1}{2}g)] \\ &= \sum_{s=0}^{\infty} K_{ss} \bar{D}_s \cos \alpha_s z \quad \text{for } 0 < z < g. \end{aligned} \quad (1.17)$$

We can solve the first two equations for \bar{A}_p by multiplying with $\exp[-ik_p(z - \frac{1}{2}g)]$ and integrating from 0 to $2\pi R$. Since the exponential function is orthogonal in that interval we find

$$\begin{aligned} \bar{A}_p + \bar{B}_p &= \alpha \sum_{s=0}^{\infty} N_{ps} \bar{D}_s + \eta_t \sum_{m=-\infty}^{+\infty} (I_{mm} \bar{A}_m + \bar{C}_m) \\ &\quad \cdot (\delta_{pm} - \alpha V_{pm}), \end{aligned} \quad (1.18)$$

where $\alpha = g/2\pi R$,

$$N_{ps} = \frac{\pi \alpha p}{(\pi \alpha p)^2 - (\pi s/2)^2} \begin{cases} \sin \pi \alpha p & s \text{ even} \\ -i \cos \pi \alpha p & s \text{ odd} \end{cases} \quad (1.19)$$

and

$$V_{pm} = \frac{\sin \pi \alpha (p-m)}{\pi \alpha (p-m)}. \quad (1.20)$$

The magnetic condition (1.17) is solved for \bar{D}_t by multiplying by $\cos \alpha_s z$ and integrating from 0 to g . Since the cosine is orthogonal in that interval we find with $\int_0^g \cos^2 \alpha_t z dz = \frac{1}{2}g(1 + \delta_{t0})$:

$$\frac{1}{2}(1 + \delta_{t0}) K_{tt} \bar{D}_t = \sum_{m=-\infty}^{+\infty} N_{mt}^* (I_{mm} \bar{A}_m + \bar{C}_m). \quad (1.21)$$

Introducing $R_{tt} = 2/(1 + \delta_{t0}) K_{tt}$ and $N_{tm}^+ = N_{mt}^*$, the Hermitian conjugate of N_{mt} , we obtain

$$\bar{D}_t = R_{tt} \sum_{m=-\infty}^{+\infty} N_{tm}^+ (I_{mm} \bar{A}_m + \bar{C}_m). \quad (1.22)$$

1.8. If we remember that the indices m and p always run from $-\infty$ to $+\infty$, and the indices s and t from 0 to ∞ , we may leave off the indices and write the equations in matrix form

$$\bar{A} + \bar{B} = \alpha N \bar{D} + \eta_t (U - \alpha V) (I \bar{A} + \bar{C}) \quad (1.23)$$

$$\bar{D} = R N^+ (I \bar{A} + \bar{C})$$

Here \bar{A} , \bar{B} , \bar{C} and \bar{D} are column vectors (\bar{B} and \bar{C} with a single nonzero element at $m=n$), and R and I are diagonal matrices (U is the unit matrix). Only the matrices N and V are full two-dimensional matrices. The elements of N are either real or imaginary because of our choice of origin along the z axis in Sec. 1.3. Eliminating \bar{D} from (1.23)

and rearranging terms we find the essential equation determining the field coefficients \bar{A}_m :

$$[U - \alpha N R N^+ I - \eta_t (U - \alpha V) I] \bar{A} \\ = [\alpha N R N^+ + \eta_t (U - \alpha V)] \bar{C} - \bar{B}. \quad (1.24)$$

1.9. The coupling impedance Z is defined as the negative ratio of the perturbed voltage—obtained by integrating the average electric field along the trajectory of a particle over one period—to the amplitude of the perturbed current in the beam.

The average of the electric field strength over the beam cross section is given by

$$\langle E_z^I \rangle = \frac{1}{\pi a^2} \int_0^{2\pi} d\phi \int_0^a E_z^I r dr \quad (1.25)$$

which becomes from (1.5)

$$\langle E_z^I \rangle = \sum_{m=-\infty}^{+\infty} \left[\bar{A}_m \frac{2I_1(\chi_m a)}{\chi_m a I_0(\chi_m b)} - \delta_{mn} \right] \\ \cdot \exp[ik_m(z - \frac{1}{2}g)]. \quad (1.26)$$

We now put back the normalising factor $i\hat{\rho}/k\epsilon_0$ and the time factor $\exp(-i\omega t)$. For a particle travelling with the perturbation we have $z - \frac{1}{2}g = \beta ct$ and hence $\omega t = k(z - \frac{1}{2}g)$. Then we find for the voltage seen by the particle in the period

$$V = \frac{i\hat{\rho}}{k\epsilon_0} \sum_{m=-\infty}^{+\infty} \left[\bar{A}_m \frac{2I_1(\chi_m a)}{\chi_m a I_0(\chi_m b)} - \delta_{mn} \right] \int_0^{2\pi R} dz \\ \cdot \exp[i(k_m - k)(z - \frac{1}{2}g)]. \quad (1.27)$$

This becomes simply

$$V = 2\pi R \frac{i\hat{\rho}}{k\epsilon_0} \left[\bar{A}_n \frac{2I_1(\chi a)}{\chi a I_0(\chi b)} - 1 \right]. \quad (1.28)$$

We notice that only the fields with the same mode number as the perturbation contribute to the coupling impedance. The amplitude of the perturbed current is $I = \hat{\rho}\beta c\pi a^2$ and hence the coupling impedance becomes

$$Z = -\frac{2i n Z_0}{\beta(ka)^2} \left[\bar{A}_n \frac{2I_1(\chi a)}{\chi a I_0(\chi b)} - 1 \right]. \quad (1.29)$$

Since $\chi a = ka/\gamma$ is small compared to unity up to high mode numbers ($n \approx \gamma R/a$) we can usually replace the Bessel functions by their small argument approximations and obtain

$$\frac{Z}{n} = -\frac{2i Z_0}{\beta(ka)^2} (\bar{A}_n - 1). \quad (1.30)$$

We calculate Z/n because this parameter is required in stability calculations. Since the real part of the impedance must be positive for passive devices, the imaginary part of \bar{A}_n will have to be positive—this is a useful check for numerical evaluations of \bar{A}_n .

2. THE COUPLING IMPEDANCE OF CORRUGATED WALLS AT LONG WAVELENGTHS

2.1. We assume that the wavelength of the perturbation is much longer than the length g of the enlarged portion of the vacuum chamber. In this case, we have $n \ll 1/\alpha = 2\pi R/g$.

First we solve the case of perfectly conducting walls in which case (1.24) takes the form:

$$(U - \alpha N R N^+ I) \bar{A} = \alpha N R N^+ \bar{C} - \bar{B}. \quad (2.1)$$

In the limit $\alpha \rightarrow 0$, corresponding to a smooth vacuum chamber, we find immediately $\bar{A} = -\bar{B}$, and hence, from (1.30).

$$Z/n = \frac{2i Z_0}{\beta(ka)^2} (\bar{B}_n + 1). \quad (2.2)$$

Substituting the definition of \bar{B} (1.16), and approximating the Bessel functions by the first two terms of their power series yields:

$$Z/n = \frac{i Z_0}{2\beta\gamma^2} (\frac{1}{2} + 2 \ln b/a), \quad (2.3)$$

in agreement with the well-known formula for the coupling impedance of a perfectly conducting cylindrical vacuum chamber.⁽¹⁾

2.2. We may write (1.24) in the new variable $\bar{X} = \bar{A} + \bar{B}$ which expresses the additional effect caused by the presence of enlarged portions of the vacuum chamber. We obtain

$$[U - \alpha N R N^+ I - \eta_t (U - \alpha V) I] \bar{X} \\ = [\alpha N R N^+ + \eta_t (U - \alpha V)] \bar{Y}, \quad (2.4)$$

where $\bar{Y} = \bar{C} - I\bar{B}$. The only nonvanishing element of the vector \bar{Y} is $\bar{Y}_n = a I_1(\chi a) / (\chi b^2 I_0(\chi b)) \approx a^2 / 2b^2$.

2.3. For small values of the circumference factor α and perfectly conducting walls with $\eta_t = 0$ the first order solution of (2.4) is simply $\bar{X} = \alpha W \bar{Y}$

where $W = NRN^+$. Hence the n th component of \bar{X} becomes $\bar{X}_n = W_{nn} \bar{Y}_n$ where

$$W_{nn} = \sum_{s=0}^{\infty} N_{ns} R_{ss} N_{sn}^+ = \sum_{s=0}^{\infty} \frac{1 - (-)^s \cos 2\pi\alpha n}{1 + \delta_{s0}} \cdot \frac{\Gamma_s b R_0(\Gamma_s b)}{R_1(\Gamma_s b)} \frac{(\pi\alpha n)^2}{[(\pi\alpha n)^2 - (\pi s/2)^2]^2}. \quad (2.5)$$

2.4. In the case of bellows, with $g \ll \pi b$, we find from (2.5), taking only the $s = 0$ term:

$$W_{nn}^{(0)} = \Gamma_0 b R_0(\Gamma_0 b) / R_1(\Gamma_0 b). \quad (2.6)$$

If $\Gamma_0 d < 1$ we may use the small argument approximations for R_0 and R_1 and obtain

$$W_{nn}^{(0)} = -(\Gamma_0 b)^2 \ln \lambda = (\beta k b)^2 \ln \lambda, \quad (2.7)$$

where $\lambda = d/b$. Substituting (2.7) into the equation for \bar{X}_n and inserting the result into (1.30), yields the contribution of bellows to the coupling impedance:

$$Z/n = -i\alpha\beta Z_0 \ln \lambda \quad (2.8)$$

valid under the assumptions $n \ll 1/\alpha$ and $\beta k d \ll 1$. Combining the effects of the smooth wall and the bellows, we find the total coupling impedance

$$Z/n = \frac{iZ_0}{2\beta} \left[\frac{1}{\gamma^2} \left(\frac{1}{2} + 2 \ln b/a \right) - 2\alpha\beta^2 \ln d/b \right]. \quad (2.9)$$

For shallow bellows with $\tau = d - b \ll b$, we may develop the logarithm and get for $\alpha = 1$:

$$Z/n = \frac{iZ_0}{2\beta} [\gamma^{-2} (\frac{1}{2} + 2 \ln b/a) - 2\beta^2 \tau/b] \quad (2.10)$$

in agreement with the coupling impedance for a fin-loaded waveguide.⁽⁶⁾

2.5. For pairs of cross-section variations, for which $g \gg \pi b$, we have to include higher order terms in the sum for W_{nn} . The simplest approach consists of using small argument approximations for R_0 and R_1 for the whole sum. The summation can then be performed and yields a first approximation to the coupling impedance:

$$Z/n = \frac{iZ_0}{2\beta\gamma^2} [(1-\alpha)(\frac{1}{2} + 2 \ln b/a) + \alpha(\frac{1}{2} + 2 \ln d/a)]. \quad (2.11)$$

This result is trivial because it is just the sum of the contributions (2.3) of the smooth chamber with radius b and circumference factor $(1-\alpha)$, and of the smooth chamber with radius d and circumference factor α .

In order to obtain a better estimate of the coupling impedance of a pair of cross-section variations, we have evaluated W_{nn} by computer. The program performs the summation (2.5) until 200 more terms change the result by less than 10^{-3} ;

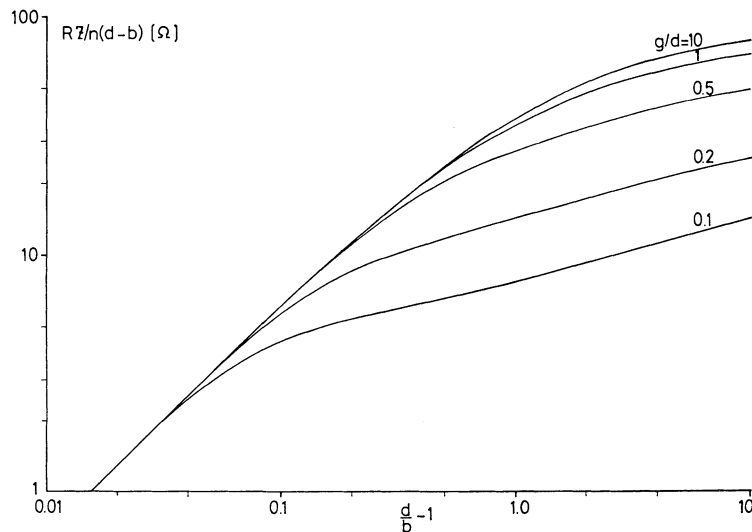


FIG. 2. Inductive coupling impedance of a pair of cross-section variations for long wavelength as function of the relative cross-section change $(d-b)/b$. The ordinate is the impedance divided by mode number Z/n , normalised with the factor $R/(d-b)$, i.e., the ratio of machine radius to cross-section change, the parameter is the "aspect ratio" g/d .

the remainder of the sum is calculated by numerical integration. Changing the switching point to 10^{-4} altered all results by less than 0.26 per cent. We write the total coupling impedance in the form:

$$Z/n = (1 - \alpha)(Z/n)_b + \alpha(Z/n)_a + (Z/n)_c \quad (2.12)$$

where $(Z/n)_b$ and $(Z/n)_a$ are the coupling impedances (2.3) of a smooth pipe of radius b and d , respectively, and $(Z/n)_c$ is the contribution of the pair of steps in cross section. The values of $(Z/n)_c$ are shown in Fig. 2 for various values of g/d . For $g/d \geq \pi$, $(Z/n)_c$ becomes independent of g and is fitted to within a few per cent by the following expression, which holds for $R \gtrsim g$:

$$(Z/n)_c = -\frac{0.241 iZ_0}{\beta R} \frac{(d-b)^2}{d+0.412b}. \quad (2.13)$$

This result differs from that for the shunt impedance of a step in the outer conductor of coaxial waveguide⁽⁷⁾ by the absence of a logarithmic term in $(d/b-1)$. This seems to be due to the different treatment of the higher space harmonics. In Ref. (7) they are treated as plane waves whereas we treat all of them exactly.

2.6. Including the finite resistivity of the outer cavity wall and the tube wall is quite straightforward. We have to solve (2.4) with $\eta_t \neq 0$. In the case of bellows ($g \ll \pi b$) we find for the total coupling impedance including resistivity:

$$Z/n = \frac{iZ_0}{2\beta} [\gamma^{-2}(\frac{1}{2} + 2 \ln b/a) - 2\alpha\beta^2 \ln d/b - (1+i)\beta^2(\alpha\delta_c/d + (1-\alpha)\delta_i/b)]. \quad (2.14)$$

The finite conductivity of the side walls of the bellows is not included here. However, a reasonably good approximation can be obtained by augmenting the resistivity of the outer wall of the bellows in the ratio of the side wall area to the outer wall area.⁽⁸⁾ For $\alpha = 0$, (2.14) agrees with the well-known expression for the coupling impedance of a resistive tube wall.⁽²⁾

3. RESONANT EFFECTS

3.1. We start again from (2.4) which we repeat below:

$$[U - \alpha NRN^+ I - \eta_t(U - \alpha V)I] \bar{X} = [\alpha NRN^+ + \eta_t(U - \alpha V)] \bar{Y}. \quad (3.1)$$

At frequencies where the enlarged portions of the vacuum chamber resonate, some elements of R and I may become very large and the approximate inversion of (3.1) used in Sec. 2 is no longer justified.

3.2. Equation (3.1) can be solved numerically when the matrices are truncated to finite size. A simple estimate shows that the size of the matrices should be much larger than the mode number n which in machines with several hundred metres circumference typically takes values of a few thousand at resonance. Even with high speed computers the inversion of matrices of this size is unpractical.

One way around this obstacle is an artificial reduction of the period length, corresponding to a smaller radius or to a large number of identical elements spaced equidistantly around the actual circumference of the machine. This method can reduce the mode number drastically and has been used successfully to find numerical solutions.⁽⁸⁾ However, it may alter the results due to the interaction between adjacent cavities.

3.3. Because of the form of the 'kernel' in (3.1) it is possible to apply a transformation which is known from the theory of integral equations. It has been shown⁽⁸⁾ that V can be expressed by the following product:

$$V = N(2U - U^0)N^+ \quad (3.2)$$

where U^0 is a matrix with elements $U_{st}^0 = \delta_{s0} \delta_{t0}$. Introducing the abbreviation $S = R - \eta_t(2U - U^0)$ we can write (3.1) in the form:

$$(U - \eta_t I) \bar{X} = \eta_t \bar{Y} + \alpha NSN^+ \bar{Y} + \alpha NSN^+ I \bar{X}. \quad (3.3)$$

We now define the new variable $\bar{X}' = SN^+ I \bar{X}$ and find:

$$[U - \alpha SN^+ I(U - \eta_t I)^{-1} N] \bar{X}' = SN^+ I(U - \eta_t I)^{-1} (\eta_t + \alpha NSN^+) \bar{Y}. \quad (3.4)$$

This equation looks very similar to (3.1). However, it has entirely different convergence properties because the order of N and N^+ in the kernel is reversed. For the numerical solution we no longer need matrices with dimensions $2\pi R/\lambda$, but only of the order g/λ , where λ is some small length inside which the field pattern around the cavity edges changes significantly. It is smaller than g , b , or

$d-b$, whichever is the smallest. In the frequency region of interest we can therefore limit ourselves to quite small matrices. The difficulty is shifted to the calculation of the elements of the kernel where we have to evaluate sums of $2\pi R/\lambda$ terms to obtain convergence. Because of the slow variation of the elements of the sum, it can fortunately often be replaced by an integral which reduces the numerical effort required.

Substitution of the solution of (3.4) into (3.3) yields after some arithmetic:

$$\bar{X} = \alpha(U - \eta_t I)^{-1} N [U - \alpha S N^+ I (U - \eta_t I)^{-1} N]^{-1} \cdot S N^+ (U - \eta_t I)^{-1} \bar{Y} + \eta_t (U - \eta_t I)^{-1} \bar{Y}. \quad (3.5)$$

3.4. We have evaluated the resonant frequency and coupling impedance of the lowest resonance which corresponds to the E_{010} mode of a cylindrical cavity, for cavities of various shapes by solving (3.5) on a computer. The only approximation in the computation is the truncation of all matrices to finite size. The number of space harmonics used is 10 in the cavity region and $(20n+1)$ in the tube region where n is the mode number. We have evaluated the truncation error by halving the size of all matrices involved. This resulted in a change of the frequency by at most 0.3 per cent, and of the coupling impedance by at most 3.5 per cent for $n=10$. The largest errors occur for extremely small and extremely large values of g/d .

For a given shape of the resonant cavity, the frequency scales as d^{-1} , and the coupling impedance and the Q value scale as $(d\sigma)^{\frac{1}{2}}$ if we assume that $\sigma_c = \sigma_t = \sigma$. Therefore, three parameters are sufficient for all possible cavity geometries: b/d , g/d and the mode number n which is closely related to the ratio $2\pi R/d$. The scaling laws were also verified by computer. In the computations we have used $d=1\text{m}$, $\gamma=30$, and $\sigma=10^6 \Omega^{-1}\text{m}^{-1}$ which corresponds to the conductivity of stainless steel. Figures 3 to 5 show the products $fd = \omega d/2\pi$, $Z(d\sigma)^{-\frac{1}{2}}$ and $Q(d\sigma)^{-\frac{1}{2}}$ for $n=10$. We have noticed that all these quantities depend very little on n once the length of the tube, $2\pi R-g$, is much longer than its attenuation length. An example of this is shown in Table I. The variation of the coupling impedance with g/d is mainly due to the transit time factor. The values of the coupling impedance for $b/d=0$ were obtained from the known formula for a closed cylindrical cavity.

TABLE I
Resonant frequency f , coupling impedance Z and quality factor Q for various mode numbers n . $a=0.01\text{m}$, $b=0.8\text{m}$, $d=1.0\text{m}$, $g=2.0\text{m}$, $\gamma=30$, $\sigma_c = \sigma_t = 10^6 \Omega^{-1}\text{m}^{-1}$, 10 space harmonics in slot region, $20n+1$ space harmonics in tube region.

n	$f[\text{MHz}]$	$Z[\text{k}\Omega]$	Q
1	118.393	25.9786	22745.
2	121.240	18.7040	21128
3	121.308	18.6755	21066
4	121.310	18.6768	21063
5	121.310	18.6765	21062
6	121.310	18.6762	21062
8	121.310	18.6757	21061
10	121.310	18.6752	21060

The dependence of the coupling impedance Z on γ is shown in Fig. 6 for a single shape of the resonant cavity. It may be seen that the coupling impedance is roughly proportional to $\beta^2 = 1 - \gamma^{-2}$. The resonant frequency and the Q factor depend on γ only very weakly.

Higher resonances can also be found by the computer program. They correspond to higher radial and axial modes of a cylindrical cavity of radius d and length g as long as the tube between the cavities is not propagating. Above the cut-off frequency of the tube a new family of modes appears.

The coupling impedance of the higher modes decreases like $f^{-\frac{3}{2}}$ if one neglects the reduction due to the transit time factor. However, it is also multiplied by a factor two for all axial modes except the lowest one. This increase is particularly noticeable for long cavities with $g/d \gg 1$ in which the axial modes are very closely spaced in frequency.

4. CONCLUSIONS

We have calculated the coupling impedance of cross-section variations for the geometrical model shown in Fig. 1. For wavelengths much longer than the dimensions of the enlarged part of the vacuum chamber the coupling impedance is essentially inductive. In a large machine like the CERN Intersecting Storage Rings (ISR) the ratio of the total inductive coupling impedance, due to a pair of cross-section variations every few metres, to the resistive coupling impedance of the stainless-steel vacuum chamber is about unity. For smaller

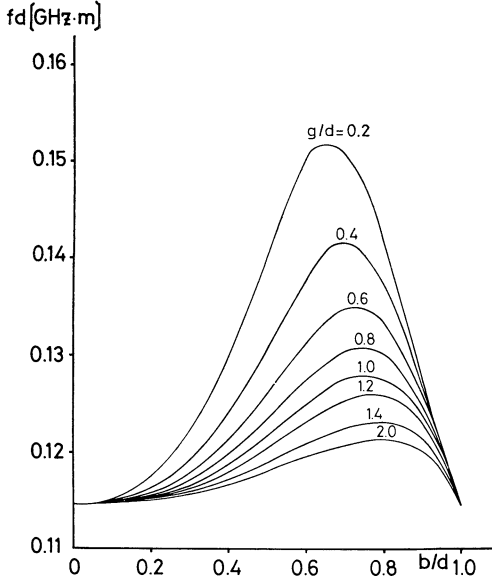


FIG. 3. Resonant frequency of the lowest mode in a cavity formed by two cross-section variations versus the relative hole-size, resp. tube diameter, b/d . The ordinate is multiplied by cavity radius d , the parameter is the aspect ratio g/d .

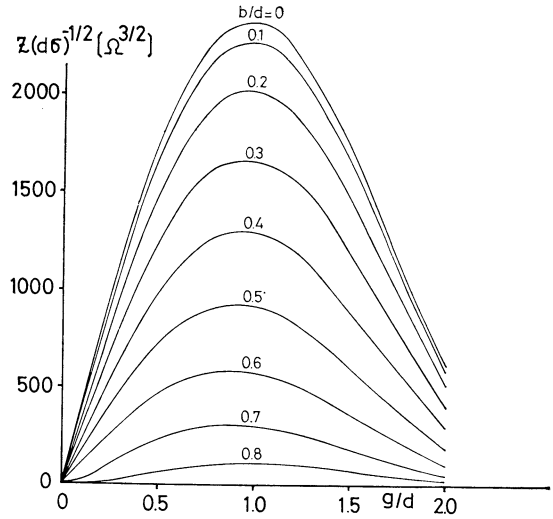


FIG. 4. Resonant coupling impedance of the lowest mode versus the aspect ratio. The ordinate is divided by the square root of the cavity radius and the wall conductivity, the parameter is the relative hole size b/d .

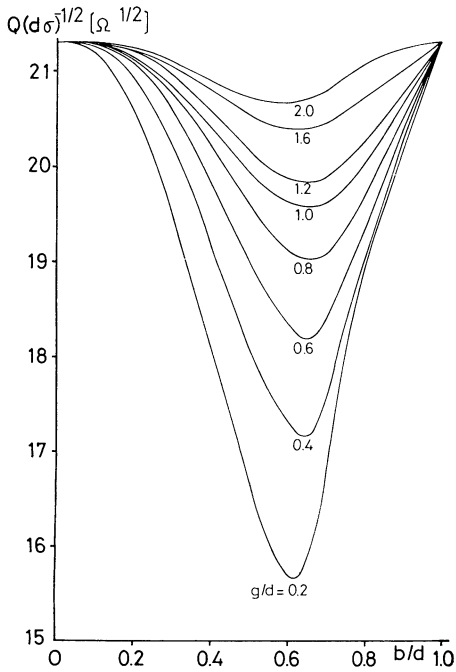


FIG. 5. Quality factor of the lowest mode versus relative hole size, divided by the square root of the cavity radius and the wall conductivity. The parameter is the aspect ratio g/d .

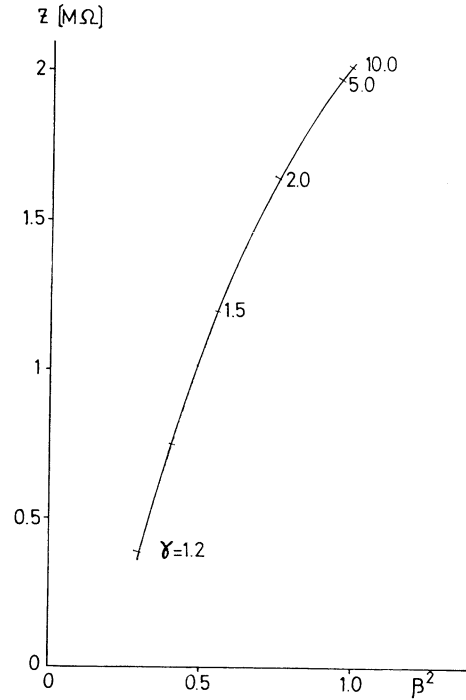


FIG. 6. Energy dependence of the resonant coupling impedance of the lowest mode in a cavity with dimensions $d = 1$ m, $g = 1$ m, $b = 0.2$ m, beam radius $a = 0.1$ m and $\sigma_c = \sigma_t = 10^6 \Omega^{-1} \text{m}^{-1}$.

relativistic machines the inductive component may exceed the resistive one as their ratio scales as $R^{-\frac{1}{2}}$.

For smaller wavelengths where the enlarged parts of the vacuum chamber form resonant cavities, the coupling impedance becomes much larger, essentially in proportion to the quality factor of the resonance. However, the presence of the tube connecting the cavities reduces the coupling impedance.

In the ISR, the shape of the vacuum chamber alternates between elliptical in the magnets and circular in the straight sections. The latter chambers form resonant cavities with $Z/n = 3.5\Omega$ each for the lowest mode, neglecting the transit time factor. Since there are about 150 of them in the machine, their total contribution will be approximately $Z/n = 500\Omega$. This figure is certainly an overestimate for the lowest mode because it assumes that all straight section chambers resonate at exactly the same frequency which will not be the case in practice. On the other hand, the next higher modes in a long cavity have coupling impedances which are nearly twice the value of the lowest resonance.

Stability criteria for the longitudinal stability of an unbunched beam in a circular accelerator or storage ring have been given in the form of upper limits on the coupling impedance.^(3,4) We use the one given in⁽⁴⁾ which is based upon realistic distribution functions⁽¹¹⁾

$$|Z/n| \lesssim \frac{E_0}{e} \frac{|\eta|}{I_0 \gamma} \left(\frac{\Delta p}{m_0 c} \right)^2, \quad (4.1)$$

where $E_0 = m_0 c^2$ is the rest energy of the particles, e is their charge, I_0 is the circulating current, γ is the energy factor, $\eta = \gamma^{-2} - \gamma_t^{-2}$ and Δp is the full width

at half height of the particle distribution function in momentum. $E_0 \gamma_t$ is the transition energy.

For the ISR a limit $Z/n = 100\Omega$ was calculated for a 2 A stack with $\Delta p/p = 10^{-3}$, and $Z/n = 1000\Omega$ for a 20 A stack with $\Delta p/p = 1$ per cent. The limits are lower than those in proton synchrotrons because of the beam manipulations associated with rf stacking. Since the resonant impedance of the straight section chambers by far exceeds the stability limit damping resistors have now been installed in one ring of the ISR.

ACKNOWLEDGEMENT

We should like to thank Miss M. Hanney and Mrs. Y. Marti for their help with the programming involved.

REFERENCES

1. C. E. Nielsen, A. M. Sessler and K. R. Symon, *Proc. Int. Conf. on High Energy Accelerators and Instrumentation, Geneva, 1959*, p. 239.
2. V. K. Neil and A. M. Sessler, *Rev. Sci. Instr.*, **36**, 429 (1965).
3. L. J. Laslett, V. K. Neil and A. M. Sessler, *Rev. Sci. Instr.*, **32**, 276 (1961).
4. E. Keil and W. Schnell, Report CERN/ISR/TH-RF/69-48 (1969), unpublished.
5. W. Schnell, Report CERN/ISR-RF/70-7 (1970), unpublished.
6. R. Briggs and V. Neil, *Plasma Physics*, **8**, 255 (1966).
7. N. Marcuvitz, *Waveguide Handbook* (McGraw-Hill, 1951).
8. E. Keil and B. Zotter, Report CERN/ISR-TH/70-30 and CERN/ISR-TH/70-33 (1970), unpublished.
9. T. Moreno, *Microwave Transmission Design Data* (McGraw-Hill, 1948).
10. B. Zotter, Report CERN/ISR-TH/70-47, (1970), unpublished.
11. A. G. Ruggiero and V. G. Vaccaro, Report CERN/ISR-TH/68-33 (1968), unpublished.

Received 19 July 1971